Practical approaches to seismic design of deep foundations

H G Poulos
Coffey Geotechnics, Australia
harry.poulos@coffey.com (Corresponding author)

Keywords: buckling; design; earthquakes; lateral response; liquefaction; pile; remedial methods

ABSTRACT

This paper sets out a simplified approach by which the practical foundation designer can undertake the relevant calculations to satisfy the requirements for deep foundation design in seismic areas. The following matters are dealt with:

a. Design issues that should be addressed;
b. Pile design for axial loading, including the possible effects of liquefaction;
c. Pile design for lateral loading where liquefaction does not occur;
d. Pile design for lateral loading where liquefaction does occur;
e. Measures to mitigate against liquefaction effects.

1. INTRODUCTION

Consideration of the effects of earthquakes and seismic loadings is an increasingly important aspect of modern foundation design, and most contemporary standards have a mandatory requirement for such consideration. For example, the Australian Piling Code, AS 2159-2009, states that "a pile shall be designed for adequate strength, stiffness and ductility under load combinations including earthquake design actions". However, the methods by which such considerations can be undertaken are generally not set out in the standards, and many approaches have been utilized, ranging from very simplistic methods to extremely complex computer analyses. Accordingly, there appears to be scope for an approach that is soundly based but which is neither too simplistic nor too complex.

Poulos (1989) has suggested that there are three categories of analysis and design, as follows:

1. Category 1: empirical methods.
2. Category 2: simplified but soundly-based methods.
3. Category 3: more comprehensive methods that are soundly-based, and site-specific.

The objective of this paper is to set out a systematic but simplified approach which falls into Category 2 above, and by which the foundation designer can undertake the relevant analyses to satisfy the foundation design requirements for seismic regions. Emphasis is placed on methods that do not require "black box" software or which employ complex soil models in which the physical meaning of the parameters is unclear.

2. DESIGN ISSUES

In addition to the conventional design issues of axial load capacity, settlement, structural adequacy and durability under static imposed loadings, the design of deep foundations in seismic areas requires consideration of the following factors:

1. The effects of earthquake excitation on the axial load capacity of the foundation system;

2. The effects of earthquake excitation on the lateral response and the structural integrity of the foundation system.

In both cases, the possible loss of soil support during the earthquake due to liquefaction or partial loss of soil strength must be considered. Both the geotechnical and the structural strength of the foundations can be compromised by the earthquake effects, and so each has to be examined in turn.

For assessment of the response of the foundation during a seismic event, it is also necessary to estimate the stiffness and damping of the foundation system, since the foundation response can influence the natural period of the supported structure.

3. EFFECTS OF EARTHQUAKES ON FOUNDATION SOILS

Soil deposits at a site subjected to an earthquake may experience the following effects:

- Increases in pore pressure within the soils;
- Time-dependent vertical ground movements during and after the earthquake;
- Time-dependent lateral ground movements during the earthquake.

In foundation design, consideration must therefore be given to possible reductions in soil strength arising from the build-up of excess pore pressures during and after the earthquake. In extreme cases, the generation of pore pressures may lead to liquefaction in relatively loose sandy and silty soils.

As a consequence of the earthquake-induced ground movements, piles and other deep foundations will be subjected to two sources of additional lateral loading:

a. Inertial loadings – these are forces that are induced in the piles because of the accelerations generated within the structure by the earthquake. Consideration is generally confined to lateral inertial forces and moments, which are assumed to be applied at the pile heads.
b. Kinematic loadings – these are forces and bending moments that are induced in the piles because of the ground movements that results from the earthquake. Such movements will interact with the piles and because of the difference in stiffness of the piles and the moving soil, there will be lateral stresses developed between the pile and the soil, resulting in the development of shear forces and bending moments in the piles. These actions will be time-dependent and need to be considered in the structural design of the piles.

Thus, in addition to the usual design considerations for static loading, the above factors of strength reduction, inertial loadings, and kinematic loadings, need to be incorporated into the design process.

When considering both the strength and stiffness of soils, consideration should also be given to the effects of the high rate of loading that occur during a seismic event. Such loading rate effects tend to increase both the strength and stiffness of soils, especially clay soils.

Appropriate assessment of the geotechnical parameters is a critical component of geotechnical design for seismic actions, as it is for other types of imposed loadings. This issue is however outside the scope of the present paper, and reference should be made to references such as Kramer (1996) who discusses such issues as the effects of strain, cyclic loading and loading rate effects.

3.1 Earthquake Characteristics Required for Foundation Design

Seismic design of foundations requires information on a number of characteristics of the anticipated earthquakes at the site, including the following:

- Earthquake size or magnitude;
- Seismicity rate;
- Maximum bedrock acceleration, and it attenuation with distance from the causative fault;
- The duration;
- The predominant period;
- Representative time-acceleration relationships at bedrock level.

More details of these and other earthquake characteristics can be found in Kramer (1996). However, interaction with seismologists is highly desirable in making the above assessments for a specific site or area.

4. PILE DESIGN FOR AXIAL LOADING

4.1 Without Liquefaction

In soils that are assessed to be non-liquefiable, the conventional methods may be adopted to assess the ultimate shaft friction and end bearing capacity of the piles, including the possible effects of group action.

Only limited attention has been paid to the axial response of piles during and after an earthquake. Poulos (1993) has provided an example of a pile in clay subjected to earthquake action. The generation of excess pore pressures, and the consequent loss of strength of the clay, has been incorporated into the analysis. The main conclusions drawn from this study are as follows:

1. Earthquakes with a Richter Magnitude in excess of about 6 have the potential to generate significant excess pore pressures in the clay, causing subsequent consolidation settlement.
2. The rate of development of these settlements is similar to that obtained from Terzaghi's consolidation theory, using the coefficient of consolidation for the soil in an over-consolidated state.
3. Piles in clay may be subjected to a short-term loss of axial capacity due to the "softening" of the surrounding soil arising from pore pressure build-up.
4. Piles may also experience a long-term increase in settlement and axial force, due to the ground settlements induced by the earthquake.

4.2 Effects of Liquefaction

If liquefaction is assessed to be likely to occur within soils supporting a piled foundation, some of the issues that require consideration are as follows:

(a) Seismic excitation will cause settlements as well as lateral ground movements and thus there will be a tendency for the development of negative skin friction on those parts of the pile which tend to settle less than the soil.
(b) There will tend to be a substantial reduction in effective stress in the soil due to the generation of excess pore pressures, and this will lead to a reduction in the lateral effective stress between the pile and the soil, and a consequent reduction in the ultimate shaft friction. This will reduce the axial capacity of the pile and the factor of safety against geotechnical pile failure. This reduction of capacity is however temporary and the initial shaft resistance should be largely re-instated after the excess pore pressures have dissipated.

To avoid temporary failure, a check should be made of the ultimate axial capacity of the pile, excluding any resistance from the liquefiable layers. Ideally, this reduced capacity should

exceed the design axial load that is likely to be applied to the pile during the earthquake by a suitable factor of safety, for example, 1.25.

An additional mode of failure, buckling of the pile, may be initiated. This matter is discussed further below.

4.3 Pile Buckling

Bhattacharya and Bolton (2004) have identified another mechanism of axial failure of piles in liquefiable soils, namely buckling under axial loading due to loss of lateral support. This mechanism is generally overlooked in design, yet can be an important contributor to foundation failure. They emphasize that buckling of a pile is an unstable and destructive failure mechanism, whereas pile bending is a more stable mechanism. Pile buckling is a possible mechanism if the following conditions exist:

- The pile is end bearing and socketed into rock;
- The pile is carrying a relatively large axial load compared to the Euler buckling load of an equivalent column.

Madabhushi and May (2009) recommend that the pile design process should incorporate the following considerations:

- The ratio of the axial load to the Euler buckling load should be limited to about 1/5 to provide a safety margin on buckling;

- The slenderness ratio of the piles, SR = $L/(I/A)^{0.5}$ (where L=effective pile length within the liquefiable layer, I = minimum moment of inertia, A = pile cross-sectional area), in the buckling zone should be no greater than 50 to avoid buckling instability.

The Euler buckling load P_E can be estimated as follows:

$$P_E = \pi^2 EI/L_e^2 \qquad (1)$$

where EI=flexural rigidity of the pile
L_e = equivalent length of pile.

The equivalent length L_e depends on the end conditions of the pile. For the extreme case of a pile head that is unrestrained against both translation and rotation, but with a fixed base, $L_e = 2L_o$, where L_o = length of pile in liquefied soil, while for a pile head that is restrained against rotation, $L_e = L_o$. Alternatively, estimates of the pile buckling load can be made using the results summarised by Poulos and Davis (1980).

5. PILE DESIGN FOR LATERAL LOADING – NO LIQUEFACTION

5.1 Assessment of Inertial Loadings

For geotechnical analysis, the inertial forces imposed on the foundation system by the structure are usually obtained by the structural designers. Broadly, the maximum lateral force on the structure is generally estimated by multiplying the mass of the structure by the peak spectral acceleration, a_{smax}. a_{smax} can be obtained most readily via the use of code-specified values for bedrock acceleration and then applying site factors to obtain surface acceleration. For a piled foundation, the lateral inertial force can be estimated as $P.a_{smax}/g$ where P = axial force on pile, and g = gravitational acceleration.

Rather than simply adopting a code-specified site factor, a site response analysis using representative earthquake records at "bedrock" level (e.g. where v_s> 750m/s) may be carried out to assess the ground response. From this analysis, response spectra can be obtained for the

acceleration versus time history at an appropriate depth in the layer, e.g. at about 1/2 to 2/3 of the pile length, to reflect the effect of the structure being founded on a pile foundation system.

If an elastic analysis is applied to the pile and a linearly varying Young's modulus with depth is assumed to apply within the soil, then the maximum bending moment due to inertial loading, M_{imax}, can be estimated approximately from the following expression given by Randolph (1981):

(a) For a free-head pile:

$$M_{imax} = 0.1 H_i L_c / \rho_c \qquad (2)$$

(b) For a fixed head pile: (fixing moment at the pile head):

$$M_{imax} = -0.1875\ H_i\ L_c\ /(\rho_c)^{0.5} \qquad (3)$$

where H_i = inertial force on pile

L_c = effective pile length = $d(E_p/G_c)^{2/7}$ (4)

G_c = average shear modulus of soil over a depth equal to the effective length of the pile

ρ_c = ratio of soil modulus at a depth of ¼ of effective length to that at a depth of ½ of the effective pile length.

5.2 Assessment of Kinematic Loading Effects

To estimate the possible additional bending moments and shears in the piles arising from the kinematic ground movements during and after a seismic event, there are at least two design approaches that may be adopted:

a. A simple approach employing the results of analyses reported by Nikolaou et al (2001), among others
b. A more detailed approach involving the use of a pseudo-static analysis in which the results of a site response analysis are combined with a pile-soil interaction analysis (e.g. Cubrinovski and Ishihara, 2004, Tabesh & Poulos, 2001).

5.2.1 Simplified Analysis Method for Kinematic Moments in Pile

A convenient design approach for estimating the maximum moment induced in a pile by kinematic bending has been provided by Nikolaou et al (2001). They found that the induced moments were a maximum at interfaces between layers of different stiffness and then undertook a series of analyses to compute the bending moment at the interface between two layers (see Figure 1). They recognised that a distinction must be made between the maximum bending moment under steady state harmonic motion and the bending moment that would be developed under transient excitation, such as during an earthquake. The latter would generally be smaller than the steady state value, which would only be developed after a very large number of cycles. This distinction was also emphasized by Sica et al (2011) and Figure 2 shows, diagrammatically, the relationship between the bending moment and the frequency ratio (ratio of the predominant frequency of the earthquake to the natural frequency of the subsoil.

The following approximate relationship was developed for the peak bending moment, M_{pk}, during the transient phase of seismic excitation:

$$M_{pk} = \eta .\ M_{res} \qquad (5)$$

where M_{res} = bending moment developed under resonant conditions

η= reduction factor to allow for non-resonant conditions.

From the results of a frequency domain analysis, Nikolaou et al developed the following fitted formula for M_{res}:

$$M_{res} = 0.042\ \tau_c\ d^3\ (L/d)^{0.30}\ (E_p/E_1)^{0.65}\ (v_{s2}/v_{s1})^{0.50} \quad (6)$$

$$\text{with} \quad \tau_c = a_s\ \rho_1\ h_1 \quad (7)$$

where d = pile diameter
L= pile length
E_p = Young's modulus of pile
E_1 = Young's modulus of upper layer
v_{s1} = average shear wave velocity in upper layer
v_{s2} = average shear wave velocity in lower layer
a_s = peak ground surface acceleration
ρ_1 = mass density of upper layer
h_1 = thickness of upper layer.

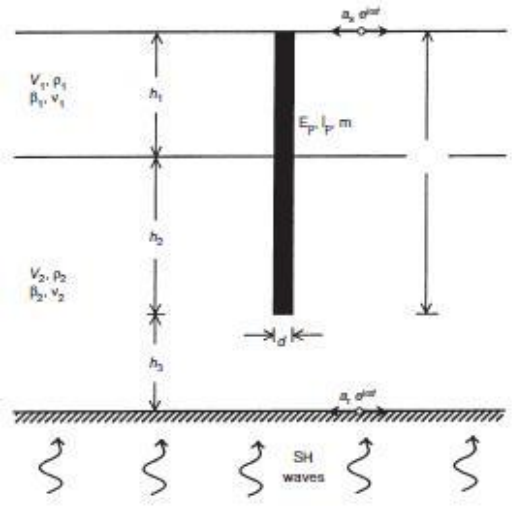

Figure 1 Model adopted by Nikolau et al (2001) for kinematic moments in pile

In the original paper, Nikolaou et al give the following expressions for the reduction factor η:

Case 1: For resonant conditions in which the fundamental period of the deposit lies within the range of predominant periods of the excitation:

$$\eta = 0.04N_c + 0.23 \quad (8)$$

Case 2: For non-resonant conditions where the fundamental period of the deposit lies outside the range of predominant periods of the excitation:

$$\eta = 0.015N_c + 0.17 \approx 0.2 \quad (9)$$

where N_c = effective number of cycles within the earthquake record.

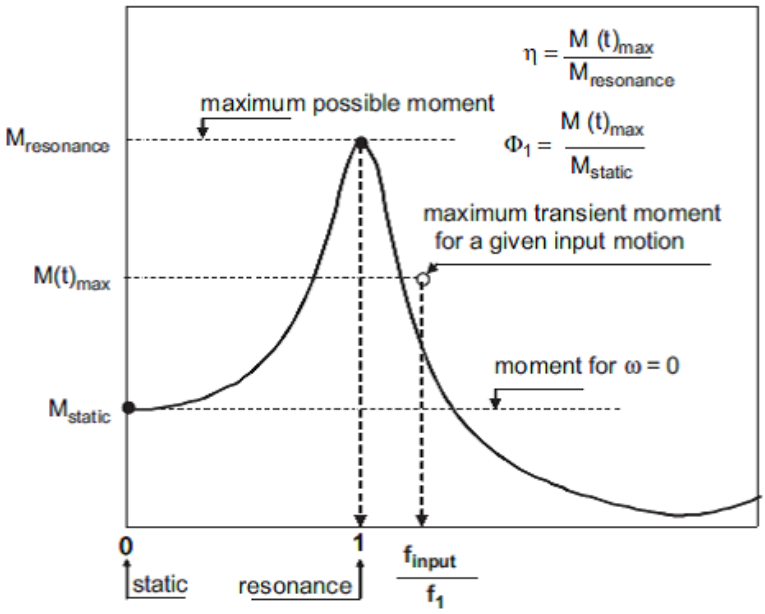

Figure 2 Relationship between pile bending moment and frequency ratio (Sica et al, 2011)

Subsequently, Sica et al (2011) have suggested the following alternative expression for the average value of η based on a series of parametric analyses:

$$\eta = 0.68(f_{input}/f_1)^{-1.5} \qquad (10)$$

where f_{input} = predominant frequency of earthquake
f_1 = natural frequency of soil profile.

The above expression holds for $(f_{input}/f_1) \geq 1.5$, but for frequency ratios less than 1.5, $\eta = 0.37$, with a standard deviation of 0.17.

The value of f_{input} can be obtained from the input earthquake record, but can also be estimated (very approximately) as the inverse of the predominant period. The value of the natural period of the soil deposit, f_1, can be obtained from the following expression:

$$f_1 = v_{sav}/4H \qquad (11)$$

where H = thickness of soil profile
v_{sav} = average shear wave velocity of soil profile.

5.2.3 Pseudostatic Analysis for Pile Response

Tabesh and Poulos (2001) have proposed a pseudostatic approach for estimating the maximum response of a pile during an earthquake. The approach involves the following steps:

1 A free field site response analysis is carried out to obtain the time history of surface motion and the maximum horizontal displacement of the soil along the length of the pile. In general, a one-dimensional analysis can be employed, using commercially available codes such as SHAKE or DEEPSOIL, or else custom codes such as ERLS (Poulos, 1991).
2 The surface motion obtained in the above step is used in a spectral analysis of a single degree of freedom system whose natural period is equal to that of the supported structure. The spectral acceleration a_{spec} is thus obtained.

3 A static analysis of the pile is carried out in which the pile is subjected simultaneously to the application of the following loadings:

(i) A lateral force at the pile head equal to a_{spec}.P, where P = vertical load acting on pile head;

(ii) The maximum ground movements along the pile length, as obtained from Step 1.

The analysis will give the maximum moment and shear force developed in the pile by the simultaneous application of the inertial and kinematic loadings.

5.3 Combined Inertial and Kinematic Effects

The approach employed by Tabesh and Poulos (2001) may be conservative as the analysis implicitly assumes that both the inertial and kinematic loadings are in phase. However, they have found that this approach gives reasonable agreement with the results of a more complete dynamic analysis, although it does tend to be conservative, and also good agreement is found when applied to a case history in Japan.

A modification has been suggested by Tokimatsu et al (2005), using the following approach to deal with combined inertial and kinematic loadings:

- If the natural period of the superstructure is less than that of the ground, the kinematic force tends to be in phase with the inertial force, increasing the stress in the piles. The maximum pile stress occurs when both the inertial force and the ground displacements take the peak values and act in the same direction. In this case, the maximum moment is the sum of the values for inertial and kinematic effects.
- If the natural period of the superstructure is greater than that of the ground, the kinematic force tends to be out of phase with the inertial force. This restrains the pile force, rather than increasing it. The maximum pile stress tends to occur when both inertial force and ground displacement do not become maxima at the same time. In this case, the maximum moment is the square root of the sum of the squares of the moments due to each effect.

The moments via this approach have been found to be in good agreement with model tests, both with and without the effects of liquefaction.

5.4 Design Charts

Using the pseudostatic approach, Tabesh and Poulos (2007) produced some simple design charts for piles within a uniform soil profile. Figure 3 shows the problem addressed and Figure 4 gives examples of these charts for the case of a 20m long pile with a vertical load corresponding to a factor of safety of 2.5 against geotechnical failure. These charts are meant to provide only a very preliminary estimate of lateral pile response.

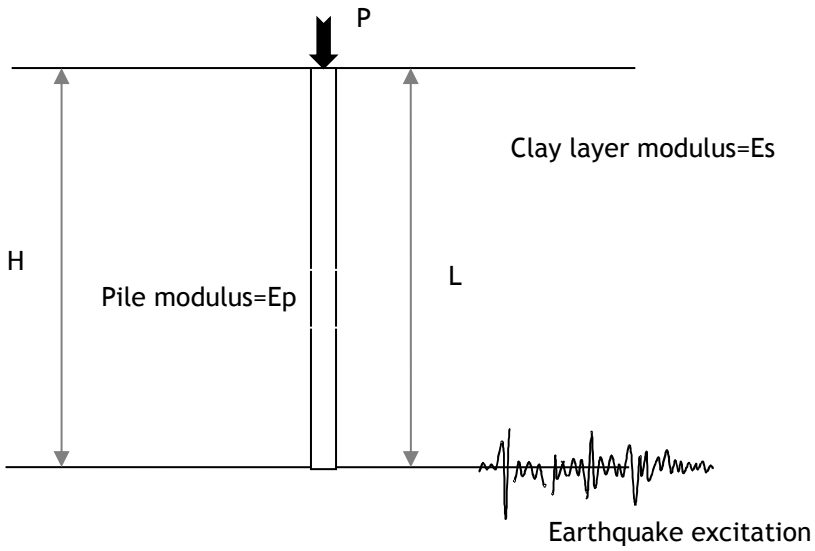

Figure 3 Problem considered for design charts

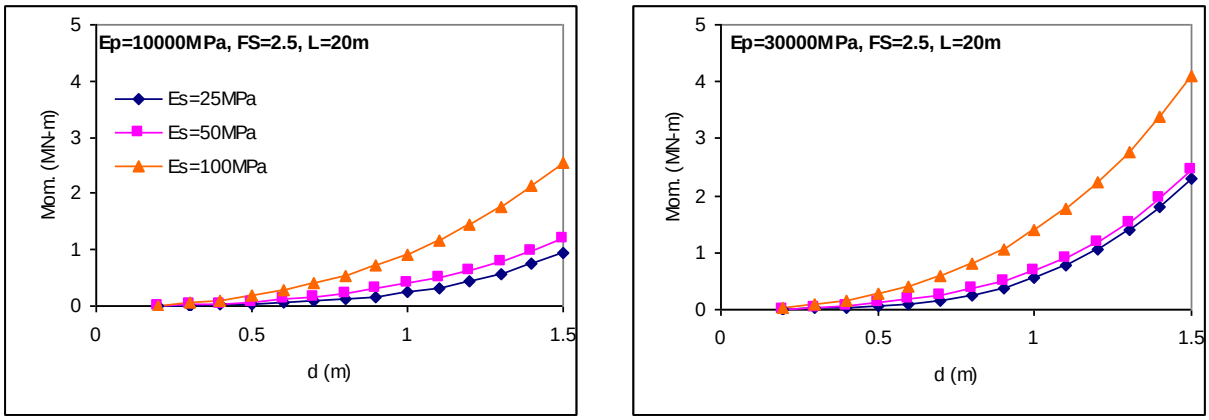

Figure 4 Typical design charts for maximum moment in 20m long pile (Tabesh & Poulos, 2007).

6. PILE DESIGN FOR LATERAL LOADING – INCLUDING LIQUEFACTION

6.1 Introduction

Soil liquefaction during a seismic event results in almost a complete loss of strength and stiffness in the liquefied soil, and consequent large lateral ground movements. The consequences of liquefaction on pile foundations can be very significant and can result in failure of the piles, as evidenced by many case histories during the 1995 Kobe earthquake (e.g. Ishihara and Cubrinovski, 1998) and the 2010-2011 events in Christchurch (e.g. Cubrinovski, 2013). A rational analysis of the behaviour of a pile in a liquefiable soil during and after an earthquake needs to take account of the effects of liquefaction on the soil properties, the natural period of the ground and the ground movements.

6.2 Simplified Analysis Based on Soil Stiffness Reduction

A procedure that has been employed in Japan to allow for the effects of liquefaction is to reduce the soil parameters by a factor which depends on the following factors:

i. The factor of safety against liquefaction, F_L;
ii. The depth below the ground surface;

iii. The original SPT (N) value of the soil.

An example of values of a reduction factor (r_k) for the modulus of subgrade reaction (k) for building foundation design in Japan is shown in Table 1 (JGS, 1998). This approach is very simplified, and considers only the effects of inertial loading. It does not incorporate the effects of kinematic loading.

Table 1 Reduction factor for modulus of subgrade reaction – building foundations (JGS, 1998)

Factor of Safety Against Liquefaction, F_L	**Depth z below ground surface (m)**	**Reduction factor r_k, applied to modulus of subgrade reaction k**			
		N≤8	**8<N≤14**	**14<N≤20**	**N>20**
≤0.5	0≤z≤10	0	0	0.05	0.1
	10<z≤20	0	0.05	0.1	0.2
0.5<FL≤0.75	0≤z≤10	0	0.05	0.1	0.2
	10<z≤20	0.05	0.1	0.2	0.5
0.75<FL≤1.0	0≤z≤10	0.05	0.1	0.2	0.5
	10<z≤20	0.1	0.2	0.5	1.0

6.3 Simplified Approach Based on Parametric Analyses

Valsamis et al (2012) have carried out an extensive set of parametric analyses and developed simplified expressions for lateral pile response in a laterally spreading soil profile. Three cases have been considered, as illustrated in Figure 5, and are as follows:

1. Case a: a 2-layer soil profile where a thick liquefiable layer overlies a non-liquefiable layer, and the pile head is unrestrained.
2. Case b: a 2-layer soil profile, as in Case a, but with the pile head restrained from both translation and rotation.
3. Case c: a 3-layer soil profile, where the liquefiable layer lies between two non-liquefiable layers, an overlying crust, and a lower continuous layer. The pile head is restrained from rotation but can translate freely.

The following expressions were derived for the maximum pile deflection, δ_{pile}:

Case a: $\delta_{pile} = \min[1.22\delta_{gr}, 29b^{1.44}.\delta_{gr}^{0.28}.J^{0.72}]$ (12)

Case b: $\delta_{pile} = \min[0.15\delta_{gr}, 0.12b^{0.74}.\delta_{gr}^{0.26}.J^{0.74}]$ (13)

Case c: $\delta_{pile} = 1.22\delta_{gr}$ (14)

where δ_{gr} = ground surface movement (m)
$J = H^6_{liq}.d/EI$
E = pile modulus (kPa)
I = pile moment of inertia (m^4)
H_{liq} = depth of liquefied soil (m)
d = pile diameter (m)
b = parameter related to corrected SPT value $(N_1)_{60,cs}$ and derived from Figure 6.

The maximum bending moment, M_{max}, is approximated by the following expressions:

Case a: $M_{max} = 2.2EI.\delta_{pile}/H^2_{liq}$ (15)

Case b: $M_{max} = 18EI.\delta_{pile}/H^2_{liq}$ (16)

Case c: $M_{max} = 17(EI.\delta_{pile}/H^2_{liq})^{0.65}$ (17)

In all cases, it is very important to use the correct units indicated above.

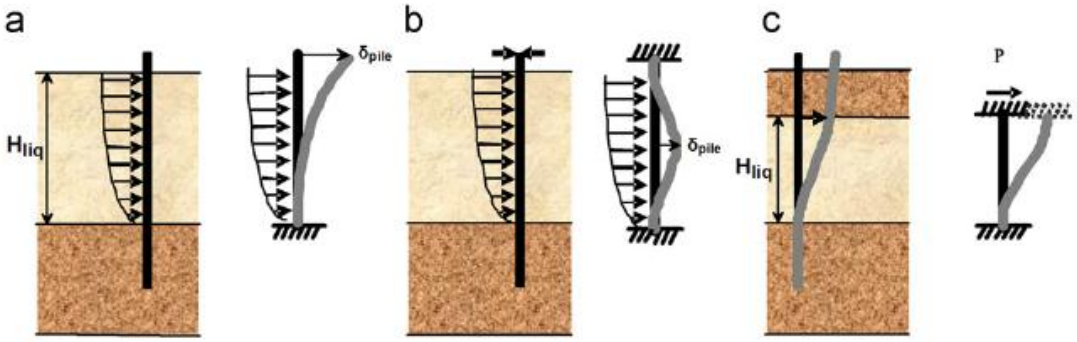

Figure 5 The design cases considered by Valsamis et al (2012)

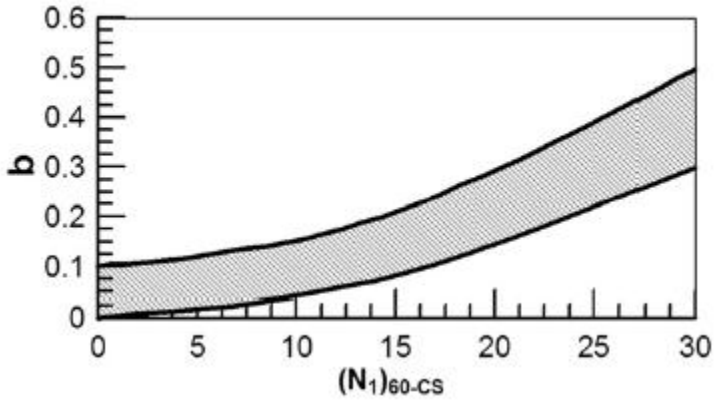

Figure 6 Parameter "b" related to corrected SPT value (Valsamis et al, 2012)

A practical difficulty with the above procedure is that the ground surface movement of a liquefied layer, $\delta_{gr,}$ is very difficult to estimate, and the computed responses depend greatly on this value.

6.4 Modified Approach Using Nikolau et al (2001)

6.4.1 Procedure

Use can be made of the equations developed by Nikolau et al (2001) to develop a simpler approach in which the amount of computational effort is relatively limited. This approach involves the following steps:

1. Estimate the reduction in shear modulus via the approach suggested by Ishihara and Cubrinovski (1998), in which the post-liquefaction shear modulus, G_{pl}, is given by:

$$G_{pl} = \beta\, G \qquad (18)$$

where β = reduction factor;
G = shear modulus prior to liquefaction.

2. Estimate the bending moment for resonant conditions via equations 6-11. The shear wave velocity in the (upper) liquefied layer is now $v_{s1\text{-}liq} = v_{s1}\sqrt{\beta}$ where v_{s1} is the original shear wave velocity of the layer.

3. Estimate the modified natural frequency of the liquefied layer from equation 11, using the reduced shear wave velocity $v_{s1\text{-}liq}$.

4. Compute the correction factor η from either equations 8 and 9, or equation 10.

5. Compute the bending moment from equation 5.

6.4.2 Modulus Reduction Factor β

A key parameter choice is the value of the modulus reduction factor β. Cubrinovski (2006) suggests that β values range between 0.02 and 0.10 for cyclic liquefaction, and 0.001 to 0.02 for lateral spreading.

An alternative approach to estimating β is to relate it to the factor of safety against liquefaction F_L, or perhaps more logically, to the liquefaction potential index LPI, which is defined as follows:

$$LPI = \int F(z)\, w(z)\, dz \qquad (19)$$

where $F(z) = 1\text{-}F_L$ when $F_L<0.95$, and F_L = factor of safety against liquefaction
$F(z) = 2x10^{-6} \exp(-18.427F_L)$ when $0.95<F_L<1.2$
$F(z)= 0$ when $F_L \geq 0$
$W(z) = 10\text{-}0.5z$
z = depth below surface in metres.

The integration in equation 19 is carried out from the surface to a depth of 20m. Table 2 summarises the general levels of risk based on LPI.

To do this, use can be made of the recommendations shown in Table 1, from which ranges of values of LPI can be obtained from the range of values of F_L given in that table for the upper 10m of the profile and profile from 10 to 20m depth. Figure 7 shows the values of the modulus reduction factor β can be plotted against the derived average values of LPI, and from this plot, an empirical relationship can be drawn as follows:

$$\beta = \beta_{lim} + e^{b.LPI}(1\text{-}\beta_{lim}) \qquad (20)$$

where β_{lim} = lower limit value of β
b = index derived from fitting through the points in Figure 7, and found to be approximately -0.20
LPI = liquefaction potential index.

This relationship is also shown in Figure 7 for b = -0.2 and β_{lim} = 0.01, and shows reasonable agreement with the points derived from Table 1, despite the considerable scatter.

Table 2: Liquefaction Risk Based on Liquefaction Potential Index, LPI

LPI	Liquefaction Risk
0	Non-liquefiable
0-2	Low
2-5	Moderate
5-15	High
>15	Very high

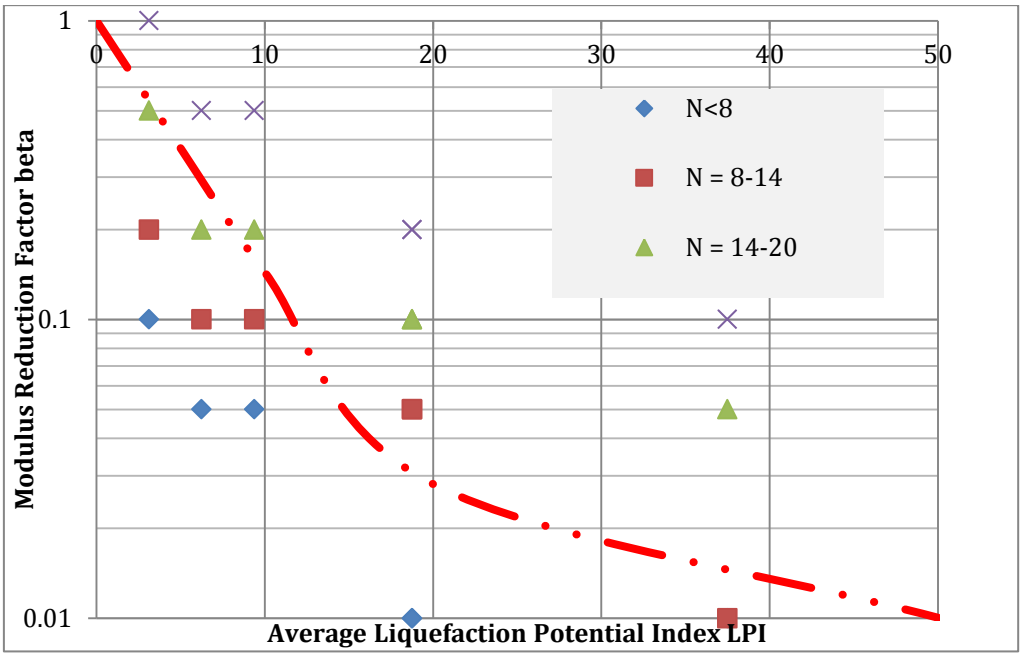

Figure 7 Relationship between modulus reduction factor b and liquefaction potential index LPI

6.4.2 Upper Limit to Kinematic Bending Moment

There will be an upper limit to the kinematic bending moment, which will occur if the layer has completely liquefied and flows past the pile. In this case (assuming that the applied pressure from the liquefied layer acts in the same direction along the whole layer), the limiting kinematic bending moment, M_{klim}, will be given by the following approximate expression):

$$M_{klim} = n.s_{u\text{-}Liq.}d\ h_1(h_1+dh) \qquad (21)$$

where n = undrained shear strength multiplier for limiting lateral pile-soil pressure
$s_{u\text{-}Liq.}$ = shear strength of liquefied soil
d = pile diameter
h_1 = thickness of liquefied layer
dh = additional distance within underlying layer at which the maximum moment occurs (typically expected to be 0.5d-1d).

Data presented by Cubrinovski et al (2009) indicate that the parameter n in equation 21 may be about 9 (i.e. 4.5 times the Rankine passive pressure).

6.4.3 Estimation of Inertial Bending Moment in Pile

In cases where complete liquefaction of the upper layer occurs, with resultant lateral spreading of the liquefied soil, it has been suggested by Klimis et al (2004) that inertial effects can be neglected. However, the analyses and comparisons carried out by Liyanapathirana and Poulos (2005) indicate that inertial effects can be present and should be considered.

Following the recommendations of Liyanapathirana and Poulos (2005), the inertial force H_i can be estimated as follows:

$$H_i = a_s . P \tag{22}$$

where a_s = peak ground acceleration;
P = vertical load acting on pile.

Assuming (albeit boldly) that an elastic analysis can be applied to a pile in a liquefied layer, and that a constant Young's modulus applies to the liquefied layer, the maximum bending moment due to inertial loading, M_{imax}, can be estimated from the following expression derived from Randolph (1981):

(a) For a free-head pile:

$$M_{imax} = 0.1 H_i (L_c + h_1) \tag{23}$$

(b) *For a fixed head pile*: Fixing moment at the pile head):

$$M_{imax} = -0.1875\ H_i (L_c + h_1) \tag{24}$$

where H_i = inertial force on pile
h_1 = depth of liquefied soil
L_c = critical pile length in the non-liquefied soil, and approximated as:
$L_c = d(E_2/G_{red})^{2/7}$
G_{red} = shear modulus of the non-liquefied layer.

6.4.4 Effect of Near-Surface Crust above Liquefiable Layer

In cases where a stiffer (and non-liquefiable) crust may exist above the liquefiable layer, account needs to be taken of the effect of the stiffness of this crust on the behaviour of the pile under inertial loading, and its effect on the limiting bending moment that can be imposed on the pile.

An approximate, but conservative, allowance for the stiffness of the crust may be made by using a weighted average Young's modulus, E_{cl}, of the crust and the liquefiable layer, as follows:

$$E_{cl} = (E_c . h_c + E_l . h_l)/(h_c + h_l) \tag{25}$$

where E_c = Young's modulus of crust
h_l = thickness of crust
E_l = Young's modulus of liquefiable layer
h_l = thickness of liquefiable layer.

The maximum inertial bending moment can then be obtained from equation (23) for a free-head pile, or equation (24) for a fixed head pile.

To obtain the maximum kinematic bending moment at the interface between the liquefiable and non-liquefiable layers, the crust should not influence this value, and the simplified approach may again be used, using as before, the modulus of the liquefiable layer G_{pl} (equation 18).
When estimating the limiting bending moment that can be imposed on the pile, an additional shear force, H_{cr} and moment M_{cr} will be applied to the pile by the crust. These can be estimated as follows:

$$H_{cr} = h_{cr}.\ p_{ucr}.d \tag{26}$$

$$M_{cr} = H_{cr}\ (h_1+0.5h_{cr} + L_c) \tag{27}$$

where h_{cr} = thickness of non-liquefied crust
p_{ucr} = ultimate lateral crust-pile pressure, and which can be estimated as approximately 4.5 times the Rankine passive pressure exerted by the crust.
d = pile diameter
h_1 = thickness of liquefied layer (below crust)
L_c = critical pile length in the non –liquefied soil layer (see equation 24).

The combination of inertial and kinematic effects can then be considered as per the recommendations of Tokimatsu et al (2005) in Section 5.3.

6.5 Pseudostatic Analyses

6.5.1 Cubrinovski et al (2009).

The model developed by Cubrinovski et al(2009) is shown in Figure 8. The soil profile contains three components:

- A surface layer or crust which does not liquefy;
- A liquefiable layer;
- An underlying base layer that does not liquefy.

Each layer is characterised by a stiffness (expressed in terms of a modulus of subgrade reaction) and a limiting pile-soil pressure. The pile is analysed as a beam-spring model, and non-linear behaviour of the pile, as well as the soil, can be incorporated into the analysis by use of a finite element approach. Account is taken of both inertial and kinematic loadings.

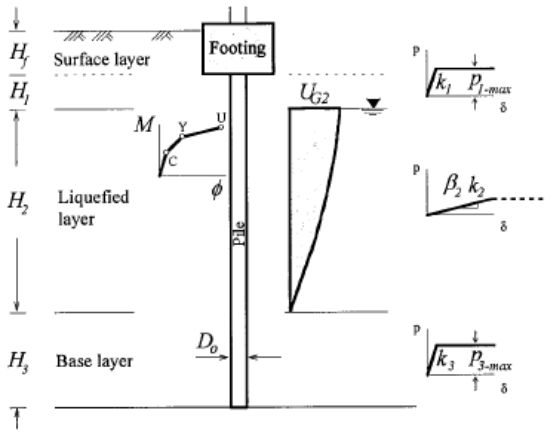

Figure 8 Model for pile in liquefied soil (Cubrinovski et al, 2009)

6.4.2 Liyanapathirana and Poulos (2005)

For piles in soils subject to liquefaction, Liyanapathirana and Poulos (2005) have developed an extension of the approach used by Tabesh and Poulos (2001) for piles in non-liquefiable soils. Account has been taken of the degradation of shear modulus of the soil that occurs with the generation of pore water pressure in the soil. The shear modulus of the soil is assumed to vary with the effective stress level of the soil as shown below:

$$G_s = G_0\left((1+2Ko)\sigma v'/\ pa\right)^{0.5}\ MPa \tag{28}$$

where $\sigma v'$ is the effective stress level of the soil, K_0 is the coefficient of earth pressure at rest, pa is atmospheric pressure, and G_0 is a constant which varies with the relative density, D_r, of the soil.

Although spectral acceleration has been used by Tabesh and Poulos (2001), it has been found that the inertial force at the pile head calculated using the spectral acceleration may overestimate the pile response when the surrounding soil starts to liquefy. Hence, the maximum acceleration at the ground surface, rather than the spectral acceleration, has been used to calculate the inertial force at the pile head.

The calculation steps involved in this approach can be summarised as below:

1. First, a free-field site response analysis is performed by taking into account the pore pressure generation and dissipation in the soil deposit due to the earthquake loading (Liyanapathirana and Poulos, 2002). From this analysis, the maximum ground surface acceleration, maximum ground displacement along the length of the pile, the minimum shear modulus and the effective stress level attained during the seismic activity can be obtained.
2. The superstructure is modelled as a concentrated mass at the pile head. Generally the superstructures supported by pile foundations are multi-degree-of-freedom systems but in the design of pile foundations, the superstructure is reduced to a single mass at the pile head to simplify the analysis.
3. The lateral force to be applied at the pile head is the cap-mass (vertical load divided by g), multiplied by the maximum ground surface acceleration obtained from the ground response analysis.
4. The pile-soil interaction is modelled using the spring coefficients calculated from elastic theory, based on the minimum shear modulus of the soil deposit at each depth, at any time, given by the free-field site response analysis (Step 1).
5. A non-linear static load analysis is carried out to obtain the profile of maximum pile displacement, bending moment and shear force along the length of the pile by applying the lateral forces calculated in Steps 3 and 4, and the soil movement profile calculated in Step 1, simultaneously to the pile.

This approach has been verified by comparison with the results of centrifuge tests (Wilson et al, 1999; Abdoun et al, 1997).

Comparisons have also been made with the field measurements made in the piles at the Pier 211 in Uozakihama Island after the Hyogoken-Nambu earthquake which occurred on 17th January 1995. Piles at bridge Pier 211 have a diameter of 1.5 m, and Figure 9 shows the crack distributions observed in piles after the earthquake. Ishihara and Cubrinovski (1998) have simulated this case, using their approach, and Liyanapathirana and Poulos (2005) also analysed it using their pseudostatic approach. The water table was 2.0 m below the ground surface and the upper 20 m of this site consisted of Masado sand with an initial shear modulus of 57.8 MN/m^2 and density of 2000 kg/m^3. Soil liquefaction was observed in the Masado sand layer below the water table only. Therefore only the top 20 m layer was analysed using the effective

stress method incorporating pore pressure generation and dissipation. After liquefaction, the effective stress level in the soil was reduced to a minimum of 2% of the initial effective overburden pressure. For this analysis the cyclic shear strength curve for the Masado sand given by Ishihara (1997) was used. It was assumed that the base rock had a density of 2200 kg/m^3 and a shear modulus of 75 GN/m^2.

Figure 9 shows the maximum bending moment profile along the pile obtained from the pseudostatic approach of Liyanapathirana and Poulos (2005), and also that calculated by Ishihara and Cubrinovski (1998). The lower end of the RC pile was assumed to be fixed while the pile head was assumed to be fixed to the footing but free to move in the horizontal direction. The predictions made by the pseudostatic approach agree reasonably well with the results given by Ishihara and Cubrinovski (1998). The yield moment for these piles is about 5 MNm. The computed maximum bending moment profile exceeds the yield moment near the pile head and in the vicinity of the boundary between the liquefied and non-liquefied layers. This is consistent with the location of cracks observed after the earthquake shown in Figure 9.

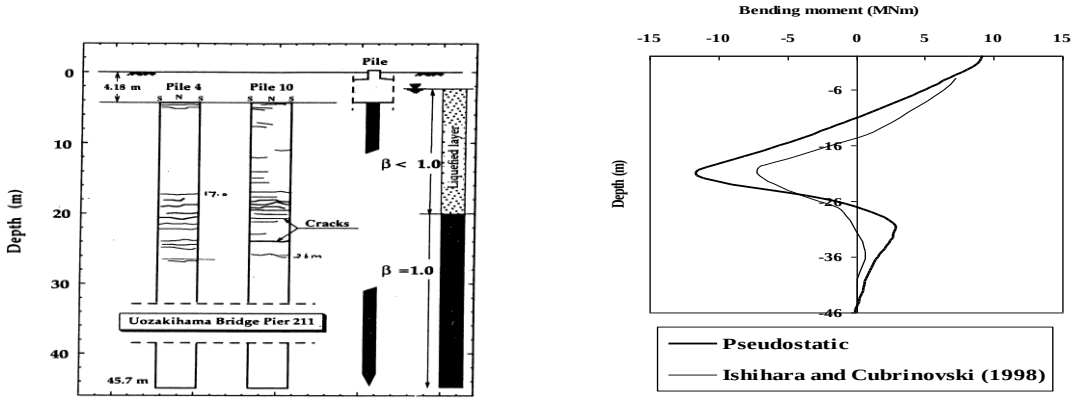

Figure 8. Cracks observed in the piles at bridge pier 211 in Uozakihama Island (Ishihara and Cubrinovski, 1998).

Figure 9 Cracks observed in piles at the bridge pier 211 in Uozakihama Island (Ishihara and Cubrinovski, 1998) and (b) Bending moment of the pile at Bridge Pier 211 in Uozakihama Island calculated from the pseudostatic approach and Ishihara and Cubrinovski (1998) results (β=0.01).

6.6 Example of Simplified Approach

To illustrate the application of the simplified approach, the above case of the bridge pile BP211 that was damaged in the 1995 Kobe earthquake (Ishihara and Cubrinovski, 1998) will be considered. The pile is one of a group of 22 bored piles, 1.5m in diameter, and is 41.5m long below the pile cap. The liquefiable layer is a reclaimed deposit 16m thick (below the pile cap) and has an average SPT-N value of about 10. The underlying layers consist of strata of sandy silt, with gravel, with SPT-N values ranging between about 10 and 50, with an average value of about 25. The average vertical load on a pile is 2.94 MN. A Young's modulus of the pile of 30000MPa will be assumed.

Using the relationship between shear wave velocity and SPT-N suggested by Imai and Tonouchi (1982), the shear wave velocity of the upper and lower layers is 173 and 234 m/s respectively, and the consequent small-strain shear moduli are 53.7 MPa and 103.9 MPa. Minimum and maximum damping ratios of 0.025 and 0.26 have been assumed for the strata at the site.
The earthquake characteristics at the site have not been documented, but based on other available information, it is assumed that the peak bedrock acceleration is 0.45g and that the predominant period of the earthquake is 1s.
Assuming that the piles have a fixed head, the inertial and kinematic maximum bending moments can be estimated for two cases:

- During the cyclic loading stage and prior to liquefaction;
- After liquefaction of the upper layer has developed.

(a) Cyclic Loading Phase

For the first case, the first step is to assess the amplification of ground motion, and based on the above assumptions, the natural period of the site is about 0.79s. Using, as an approximation, the classical expression for amplification of uniform harmonic motion, the ratio of predominant period to natural period is about 1.27, and for a damping ratio of 0.025, the amplification factor is found to be 2.64. Thus, the peak ground surface acceleration is estimated to be 0.45*2.64 = 1.188g. Using the small-strain modulus values, the following maximum moments are computed:

Inertial: -7.65 MNm (using equation 24)
Kinematic: 3.10 MNm (using the method of Nikolau et al, 2001, equations 5 to 9).

(b) Post-liquefaction phase

The small-strain modulus is used for the lower non-liquefiable layer, but a degraded modulus is used for the liquefied layer. To obtain this degraded modulus, given that liquefaction did indeed occur, a Liquefaction Potential Index, LPI, of 50 can be used. From equation 20, the reduction factor β is 0.01 (the limiting value assumed). The corresponding value of shear modulus is 0.54 MPa. The site period now becomes 1.10s, while the damping ratio has increased to its assumed maximum value of 0.26. Accordingly, the amplification factor from the classical dynamic theory decreases from 2.64 (for no shear modulus degradation) to 1.64 (for LPI=50), and the peak ground acceleration is then 0.45*1.64 = 0.738g.

From the expressions for inertial and kinematic bending moments (equations 24 and 5 to 9), the following values are obtained:

- Inertial moment (at pile head): -11.96 MNm
- Kinematic moment: 121.1 MNm.

However, a check needs to be made with the limiting kinematic bending moment that can occur when the liquefied layer flows past the pile. Adopting an undrained shear strength of 3 kPa for the liquefied soil, the limiting bending moment is found, from equation 27, to be 12.3 MNm. It is clear that the assumption of elastic behaviour in the Nikolau et al method (giving a huge kinematic moment of 121.1 MNm) is not valid in this case.

The values obtained from this simple analysis compare reasonable well those reported by Liyanapathirana and Poulos (2005) (approximately -9 MNm at the pile head and about 12 MNm at the base of the liquefied layer). Ishihara and Cubrinovski (1998) incorporated pile cracking into their analysis, and their computed maximum moments of about 7MNm reflect the occurrence of pile cracking, which limited the moment that could be induced in the piles. Figure 9 shows details of two piles that were excavated and shows the cracks in the piles at or near these two locations.

Most importantly, the simplified analysis indicates that large moments would have been generated at both the pile head and at the interface between the liquefied and non-liquefied layer.

6.7 Group Effects

Under inertial loading, it is now well-recognised that group effects are detrimental in that they tend to reduce the stiffness of piles within the group and decrease the overall group capacity. Methods of dealing with these effects are given by Poulos and Davis (1980) and Fleming et al (2009).

Under kinematic loading, group effects however tend to be beneficial, due to the "shielding" action of the piles. In particular, inner piles within a group tend to be subjected to smaller forces and moments developed by ground movements than outer piles, and all piles in the group tend to experience less effect than a single isolated pile. As a consequence, the consideration of a single isolated pile will generally be conservative when considering kinematic effects.

Towhata (2008) has presented an approximate approach for estimating the reduction in lateral earth pressure on a pile due to soil movement or flow past a group of piles. This reduction can be expressed in terms of two components:

1) A "shadow factor" which reduces the "downstream" pressure by a factor of 0.8 for each successive row of piles;
2) A spacing factor, α_p, which can be expressed as follows:

(i) For a non-liquefied layer:

$$\alpha_p = (0.877(1-\eta)f) / (0.877\eta + 0.123) + 1.0 \qquad (29)$$

where $f = 1.0$ when $h_l/d \leq 3.8$
$f = 14[1/(h_l/d)^2] + 0.03$ when $h_l/d > 3.8$
h_l = depth of flowing soil
d = pile diameter
η = ratio of pile diameter to pile spacing (d/s).

(ii) For a liquefied layer:

$$\alpha_p = 1 / (0.599\eta + 0.401) \qquad (30)$$

For practical use, it is convenient to derive a group reduction factor for the pressure developed by moving soil. If, from a practical viewpoint, s/d = 20 is considered as being sufficiently widely-spaced to represent a single pile, then the Group Reduction Factor for Pressure, RFp, can be defined as:

$$RFp = \alpha_p / \alpha_p \ (s/d=20) \qquad (31)$$

Figures 10 and 11 plot the resulting values of RFp for the non-liquefied and liquefied soil cases. The beneficial effects of group action can clearly be seen from these figures. For the non-liquefied case, the effects of grouping become increasingly beneficial as the ratio h_l/d decreases, i.e. as the thickness of the moving soil decreases relative to the pile diameter.

When both inertial and kinematic effects are present, the group effects may tend to counteract each other.

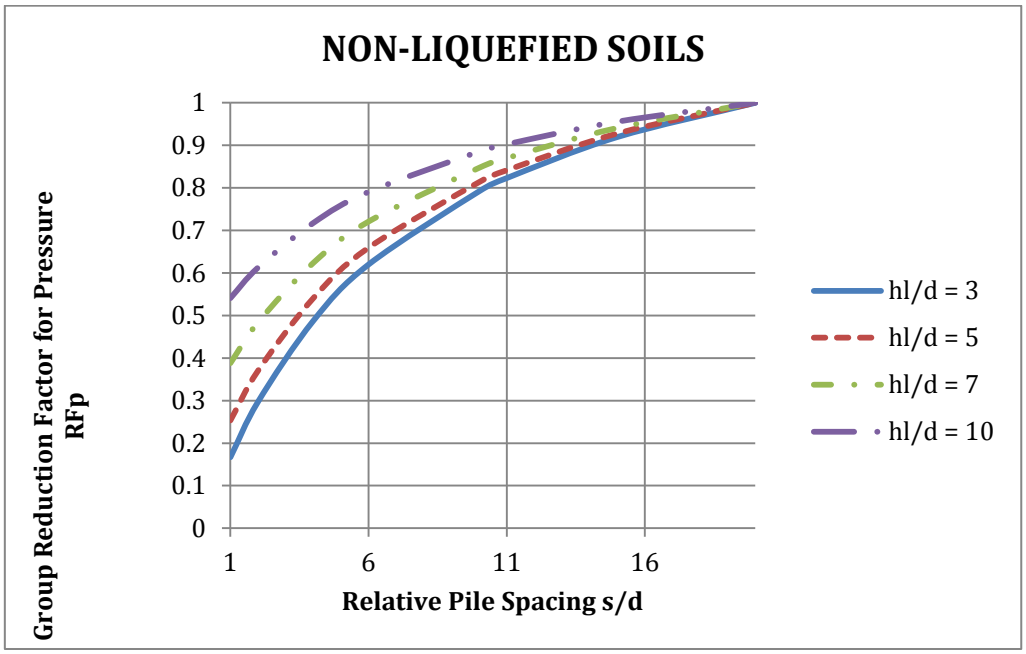

Figure 10 Group reduction factor for lateral pile-soil pressure – non-liquefied soil

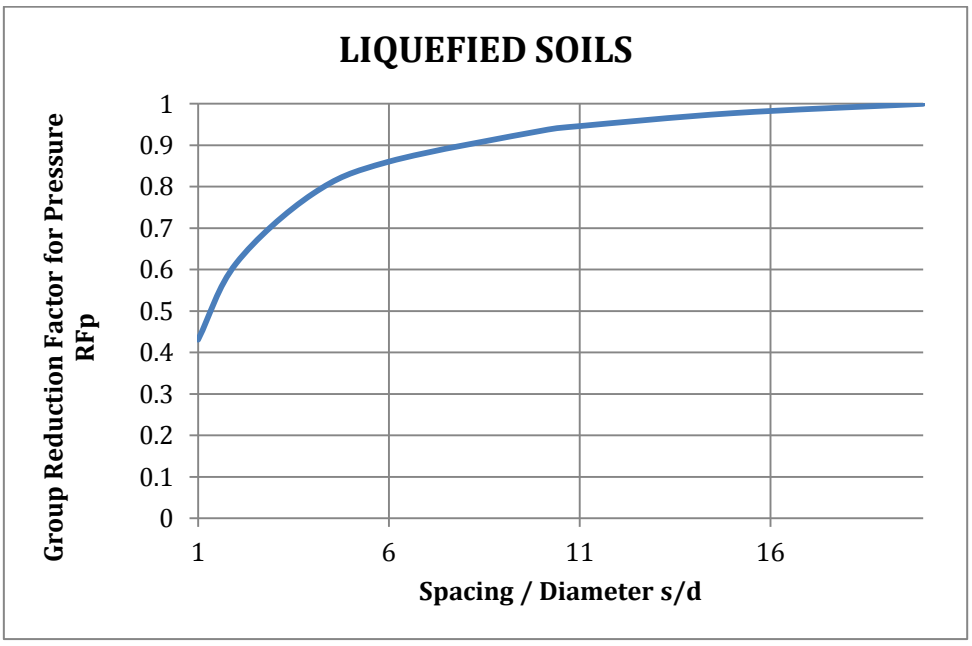

Figure 11 Group reduction factor for lateral pile-soil pressure – liquefied soil

7 FOUNDATION STIFFNESS AND DAMPING

Piles will experience vertical and horizontal movements during an earthquake due to the inertial loadings imposed by the supported structure. These movements will generally be dynamic in nature and therefore it is necessary to consider the pile head stiffnesses under dynamic loading, and the damping that will be generated by the dissipation of energy away from the piles into the surrounding soil (the radiation damping). Knowledge of foundation stiffness and damping is also required to assess the effects of structure-foundation interaction on the natural period and damping of a structure.

Theoretical solutions for the axial and lateral stiffnesses of a single pile have been provided by Novak (1987) among others. Convenient approximate solutions have been given by Gazetas (1991) for various simplified soil profiles.

In contrast to static loading, where the interaction factors between piles decrease with increasing distance between the interacting piles, the dynamic interaction factors can either increase or decrease, depending on the frequency of the loading and the spacing between the piles. It is possible that the interaction factors can be negative under some circumstances, so that group effects may possible lead to an increase in stiffness of the piles within a group, as compared with the case of static loading, where group effects generally reduce the stiffness of piles in the group. For practical design, it may often be more convenient to simplify the group as an equivalent pier, and then to use the corresponding solutions for stiffness and damping as given by Gazetas (1991).

8 MITIGATION OF LIQUEFACTION EFFECTS

8.1 Categories of Mitigation Measures

Conventional remedial measures to mitigate the effects of liquefaction can be divided into three broad categories (JGS, 1998):

- Treatment of the liquefiable soil to strengthen it;
- Treatment of the soil to accelerate the dissipation of seismically-induced excess pore pressures;
- Measures to reduce liquefaction-induced damage to the structure or facility.

8.2 Conventional Measures to Strengthen the Liquefiable Soil

An extensive discussion of measures that can be used to strengthen liquefaction-susceptible soils is given in JGS (1998). Some of the more common measures are as follows:

- Soil densification, by a variety of means, e.g. vibroflotation, blasting;
- Insertion of stiffer columns;
- Provision of drainage via stone columns.

A major limitation of all of these methods is that they cannot be used to remediate sites on which structures or facilities already exist. A number of the methods for soil densification may also not be feasible if the site is within a commercial or residential area, because of the noise and vibrations involved.
Methods involving the insertion of stiffer columns can be effective and generally involve less noise and vibration than conventional methods of densification.

8.3 Conventional Measures to Accelerate Excess Pore Pressure Dissipation

The use of stone columns or gravel drains to accelerate pore pressure drainage was developed by Seed and Booker (1977) and has been used successfully in a number of cases. In the design of stone columns for liquefaction mitigation, it is common to specify a limiting maximum pore pressure ratio (excess pore pressure divided by vertical effective stress), and this is often taken as 50%. The required length of the columns will depend on the depth of the liquefiable layer, while the required spacing of the columns will depend on the following factors:

1. The specified maximum pore pressure ratio;
2. The permeability and compressibility of the liquefiable layer;
3. The earthquake duration;
4. The equivalent number of cycles of loading from the earthquake;
5. The number of cycles to cause liquefaction;
6. The column diameter;
7. The finite permeability of the column and the effects of well resistance.

8.4 Mitigation Measures for Pile Foundations

Sato et al (2004) have suggested various countermeasures for pile foundations subjected to lateral flow of liquefiable soils. Three of these measures are illustrated in Figure 12.

The "drain piles" method aims to prevent the liquefaction of the lower layers while reducing the stiffness of the stiffer crust above the liquefiable layers. The drain piles should extend only about half-way into the upper crust, and the permeability of the drain piles should be greater than that of the liquefiable layers so that the excess pore pressures that are generated are transmitted to the upper layer. In the "earth retaining wall" method, an earth retaining wall is constructed in front of the pile foundation, to block the lateral flow. The "streamlined shield block" method involves the casting of an angled face on the upstream side of the pile cap. This angled face is meant to disperse the flowing soil and reduce its effect on the foundation.

Centrifuge tests were carried out by Sato et al (2004) to examine the effectiveness of the above countermeasures. Figure 13 summarises the test results and indicates that the "streamlined shield block" method is very effective in reducing the residual lateral displacement, and also the bending strain in the piles. It has the advantage of not requiring any ground improvement.

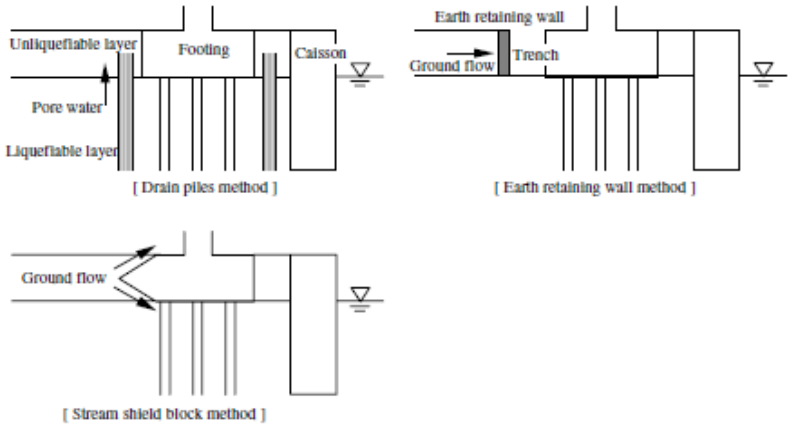

Figure 12 Countermeasures for lateral ground flow (Sato et al, 2004)

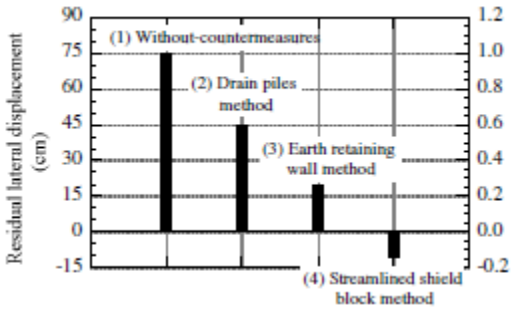

Figure 13 Measured residual lateral movements for various countermeasures (Sato et al, 2004)

8.5 Some Innovative Methods for Liquefaction Risk Mitigation

There are a number of recent innovative methods that have been explored for reducing the risk of liquefaction, several of which have the potential to be used for sites on which structures or facilities exist. A brief review of some of these methods is given below.

8.5.1 Passive Remediation via Infusion of Colloidal Silica

Colloidal silica is a dispersion of silica particles in water. With about 5% weight of silica, a colloidal silica aqueous dispersion has density and viscosity values that are similar to water, and this dispersion becomes a permanent gel abruptly after a period of time, generally a few months at most. Colloidal silica is non-toxic, biologically and chemically inert, and relatively durable. The influence of the gel is to reduce the strains in the treated soil developed by cyclic loading, and to reduce the soil permeability.

Figure 14 shows results of cyclic triaxial tests on Monterey sand, both untreated, and treated with 10% colloidal silica. The increased resistance to liquefaction is very clearly demonstrated in this figure.

Gallagher et al (2007) have described field tests to assess the performance of a dilute colloidal silica stabilizer in reducing the settlement of liquefiable soils. Slow injection methods were used to treat a 2m thick layer of liquefiable sand, using eight injection wells around the perimeter of a 9m diameter test area. The gel times ranged between 10 and 30 days. A subsequent blasting test revealed that the settlement of the treated soil was only about 60% that of an adjacent untreated area. Interestingly, there appeared to be no significant increase in the CPT resistance or the shear wave velocity, and the mechanism of improvement was considered to be due to the development of cohesion within the treated soil due to the formation of interparticle siloxane bonds.

Gallagher and Lin (2009) demonstrated that colloidal silica could be successfully delivered through 0.9m diameter columns packed with loose sand. The main factors influencing the transport of the stabilizer were the viscosity of the colloidal silica stabilizer, the hydraulic gradient, and the hydraulic conductivity of the liquefiable soil.

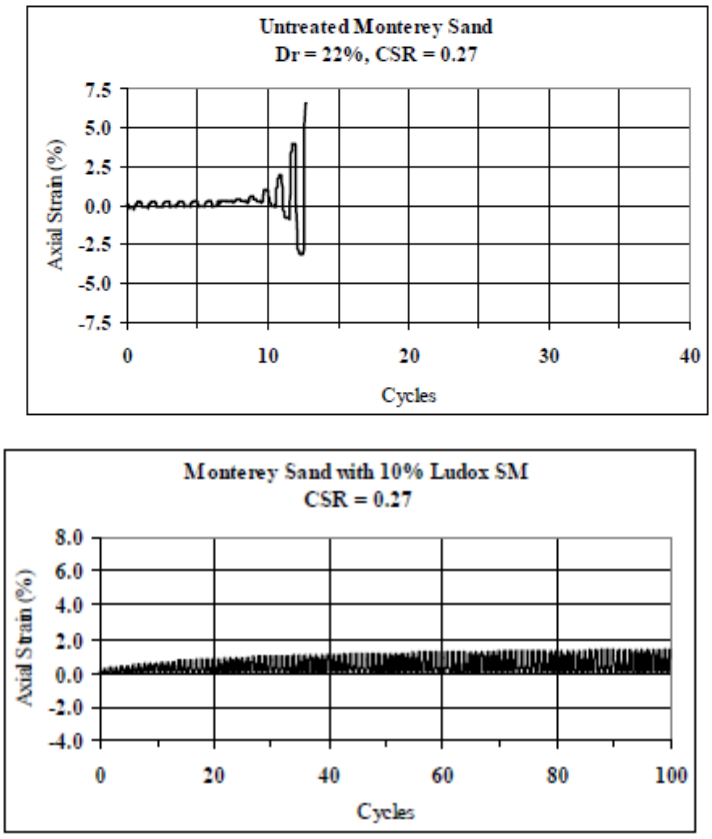

Figure 14 Comparison between cyclic behaviour of untreated sand and sand treated with 10% colloidal silica (Gallagher 2000).

8.4.2 Biogeochemical Remediation

Over the past decade, new biogeochemical techniques have been explored for the improvement of ground properties. DeJong et al (2011) summarise some of these techniques, and at least two of these have the potential to improve the liquefaction resistance of soils. The first of these involves the use of microbes to induce calcite precipitation between soil particles. The second involves the use of microbes to generate small gas bubbles within the soil and thus increase the resistance to liquefaction.

Microbially Induced Calcite Precipitation (MICP) occurs through a variety of microbiological processes, such as urea hydrolysis and denitrification. The process of calcite precipitation appears to have been discussed initially by van Meurs et al (2006), using the terms "smart soils" and "biogrout". In Biogrout, specific bacteria create a reaction which results in the precipitation of calcium carbonate in the form of crystalline calcite on the surface of the sandy particles (see Figure 15). When this reaction occurs under the right conditions, crystals are formed between two adjacent particles, producing a connection between them. This connection increases the strength and stiffness of the soil. The longer the nutrients, bacteria and reactants are present, the thicker the layer of mineralization. An important characteristic of this process of cementation is that the permeability of the porous material only reduces slightly. The biomineralization process progresses slowly in natural circumstances, but the rate of mineralization can be enhanced by stimulating the conditions.
Test data presented by Meurs et al indicated that the strength of a treated sand could be increased by a factor of almost 5, while the stiffness was increased by a factor of 3.

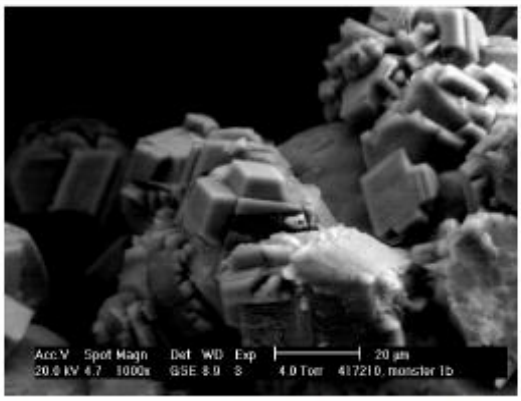

Figure 15 Scanning electron micrograph showing the mineralization of calcite onto sand grains.

DeJong et al (2010) provide a more detailed description of the process of calcite precipitation and its consequences on the geotechnical properties of the treated soil. Significant increases can be obtained in both strength and stiffness, and the volumetric behaviour can be altered from contractive to dilative, thus improving the resistance to liquefaction.

DeJong et al (2011) point out that there are a number of major challenges in implementing MICP technology. One is related to upscaling to a field scale, with issues related to cost, the stimulation of native biota, the uniformity of treatment, and the management of potentially harmful by-products. Another issue relates to the alternatives of employing bio-stimulation of native bacteria species, or the augmentation of a specific species of bacteria for a treatment zone. They suggest that bio-stimulation may be the preferred approach. A further issue may be the longevity of the treated soils, which is related to the pH of the groundwater. Tests suggest that MICP products will remain stable provided that the pH remains above 6.3.

With respect to the second technique involving microbial gas generation, Chu et al (2011) discuss some types of microorganisms that may contribute to biogas effects. This latter approach, sometimes referred to as the "Induced Partial Saturation" technique, involves the injection of non-hazardous chemicals into the ground to create gas bubbles and hence to reduce saturation. This in turn reduces the potential for liquefaction. This again has the potential to be used to improve liquefaction resistance below existing structures and buildings.

Updated information on bio- and chemo-mechanical processes in soils is provided in Geotechnique (2013).

9. CONCLUSIONS

This paper has provided a review of practical methods of assessing the effects of seismic events on the behaviour of piles, and thereby, a means of designing the piles to resist seismically-induced actions. Consideration has been given to both axial and lateral effects on piles, and for cases involving no liquefaction and also where liquefaction is assessed to occur.

In cases where liquefaction may occur, consideration needs to be given to the following issues:

1. Temporary loss of axial load capacity;
2. The possibility of axial buckling of the pile;
3. Bending moments and shears developed in the pile due to both inertial and kinematic loadings;
4. The possible beneficial effects of group action in reducing kinematically-induced bending moments.

It has been demonstrated that bending moments are likely to be a maximum at or near soil layer interfaces where there is a significant difference in the stiffness of the layers. An important case is at the junction between liquefied and non-liquefied layers. A further consequence of this behaviour is that large bending moments may occur well below the pile head, where it has been customary in the past to reduce or eliminate reinforcement in concrete piles because the moments due to inertial loads have become small. Unfortunately, in cases of earthquake loading, the kinematically-induced moments may be substantial at depth if the soil is layered and the stiffness of adjacent layers differs markedly.

There are a number of methods available for mitigating the effects of liquefaction. While some of the more traditional methods may be suitable for green-field sites, they may not be feasible for existing sites. In such cases, some of the more recent innovative methods involving bio-geo-chemical processes hold considerable promise, provided that they can be demonstrated to be economically feasible at field scale.

REFERENCES

Abdoun, T., Dobry, R. and O'Rouke, T.D. (1997). "Centrifuge and Numerical Modelling of Soil-Pile Interaction During Earthquake Induced Soil Liquefaction and Lateral Spreading." *Observation and Modelling in Numerical Analysis and Model Tests in Dynamic Soil-Structure Interaction Problems – Proceedings of Sessions held in conjunction with Geo-Logan '97,* Logan Utah, 76-90.

Bhattacharya, S. and Bolton. M. (2004). Errors in design leading to pile failures during seismic liquefaction. *Proc. 5th Int. Conf. Case Histories in Geot. Eng.*, New York, Paper No. 12A-12.

Chu, J., Ivanov, V., He, J., Naemi, M., Li, B. and Stabnikov, V. (2011). Development of microbial geotechnology in Singapore. *Proc. Geo-Frontiers 2011 Conf., ASCE Conf. Proc.* Doi:10.1061/41165:397-416.

Cubrinovski, M. (2013). Liquefaction-Induced Damage in the 2010-2011 Christchurch (New Zealand) Earthquakes. *Paper EQ-1, 7th Int. Conf. Case Histories in Geot. Eng., Chicago*, CD Volume, ISBN #1-887009-17-5.

Cubrinovski, M. and Ishihara, K. (2004) Simplified Method for Analysis of Piles Undergoing Lateral Spreading in Liquefied Soils. *Soils and Foundations* 44(5): 119-133.

Cubrinovski, M., Ishihara, K. and Poulos, H.G. (2009). Pseudo-static Analysis of Piles Subjected to Lateral Spreading. *Bull. New Zealand Soc. Earthqu. Eng*., 42(1): 28-38.

DeJong, J.T., Mortensen, B.M., Martinez, B.C. and Nelson, D.C. (2010). Bio-remediated soil improvement. *Ecological Engineering*, 36: 197-210.

DeJong, J. T., Mortensen, B., Soga, K. and Kavazanjian, E. (2011). Harnessing in-situ biogeochemical systems for "natural" ground improvement. *Geo-Strata, ASCE* GeoInstitute, July/August 2011, 36-39.

Gallagher, P.M., Conlee, C.T. and Rollins, K.M. (2007). "Full-scale field testing of colloidal silica grouting for mitigation of liquefaction risk". *J. Geotech. & Geoenv. Eng., ASCE*, 133(2): 186-196.

Gallagher, P.M. and Lin, Y. (2009). Colloidal silica transport through liquefiable porous media. *J. Geotech. & Geoenv. Eng., ASCE,* 135(11): 1702-1712.

Gazetas, G. (1991). "Foundation vibrations". Chapter 15 of Foundation Engineering Handbook, 2nd Ed., Edited H.S. Fang, Chapman and Hall, New York, 563-593.

Geotechnique (2013). Symposium in Print. Bio- and Chemo-Mechanicsl Processes in Geotechnical Engineering". *Geotechnique,* 53(3).

Imai and Tonouchi (1982). Correlation of N-value with s-wave velocity and shear modulus, *Proc. 2nd European Symp. on Penetration Testing*, 67-72.

Ishihara, K. and Cubrinovski, M. (1998). Performance of large-diameter piles subjected to lateral spreading of liquefied soils. *Keynote lecture, Proc. 13th Southeast Asian Geotech. Conf.*, Taipei, 2: 13-26.

Ishihara, K. (1997). Geotechnical aspects of the 1995 Kobe earthquake. *Terzaghi Oration, Proc. 14th Int. Conf. Soil Mechs. Foundn. Eng*., Hamburg, 4: 2047-2073.

JGS (1998). *Remedial measures against liquefaction.* Ed. Japanese Geotechnical Society (JGS). Balkema, Rotterdam.

Klimis, N., Anastasiadis, A., Gazetas, G. and Apostolou, M. (2004). "Liquefaction risk assessment and design of pile foundations for highway bridge". *Proc. 13th World Conf. Earthquake Eng.*, Vancouver, Canada, Paper No. 2973.

Kramer, S.L. (1996). *Geotechnical Earthquake Engineering.* Prentice Hall, New Jersey.

Liyanapathirana, S. and Poulos, H.G. (2002). Numerical simulation of soil liquefaction due to earthquake loading. *Soil Dynamics and Earthquake Eng*., 22: 511-523.

Liyanapathirana, S. and Poulos, H.G. (2005). Pseudostatic approach for seismic analysis of piles in liquefying soil. *Jnl. Geot. & Geoenv. Eng., ASCE,* 131(12): 1480-1487.

Madhabhushi, S.P.G. and May, R. (2009). *Pile foundations*. Chapter 9 of Seismic Design of Buildings to Eurocode 8, A.Y. Elghazouli (Ed), Spon Press, London.

Nikolaou S., Mylonakis G., Gazetas G. and Tazoh T. (2001) Kinematic Pile Bending during Earthquakes: Analysis and Field Measurements. *Geotechnique,* 51, 425−440.

Novak, M. (1987). State of the art in analysis and design of machine foundations". *Soil Structure Interaction,* Elsevier/CML Publ, New York, 171-192.

Poulos, H.G. (1989). Pile Behaviour – Theory and Application. *29th Rankine Lecture, Geotechnique,* 39(3): 365-415.

Poulos, H.G. (1991). *ERLS User's Manual.* Coffey Partners International, Sydney.

Poulos, H.G. (1993). Effect of earthquakes on settlements and axial pile response in clays. Aust. *Civil Eng. Transactions, IEAust,* Vol. CE35(1): 43-48.

Poulos, H.G. and Davis, E.H. (1980). *Pile foundation analysis and design*. John Wiley, New York.

Randolph, M.F. (1981). The response of flexible piles to lateral loading. *Geotechnique*, 31(2): 247-259.

Sato, K., Higuchi, S. and Matsuda, T. (2004). A study of the effect of countermeasures for pile foundation under lateral flow caused by ground liquefaction. *Proc. 13th World Conf. Earthquake Eng.*, Vancouver, Paper No. 452.

Seed, H.B. and Booker, J.R. (1977). Stabilization of potentially liquefiable sand deposits. *Jnl. Geot. Eng., ASCE*, 103(GT7): 757-768.

Sica S., Mylonakis G., Simonelli A.L. (2011) Transient kinematic pile bending in two layer soils. *Soil Dynamics and Earthquake Engineering* , Vol. 31, pp. 891-905.

Tabesh, A. and Poulos, H.G. (2001). Pseudostatic approach for seismic analysis of single piles. *Jnl. Geot. & Geoenv. Eng., ASCE*, 127(9): 757-765.

Tabesh, A. and Poulos, H.G. (2007). Design Charts for Seismic Analysis of Single Piles in Clay. *Proc. ICE, Geotechnical Engineering*, 160(GE2): 85-96.

Tokimatsu, K., Suzuki, H. & Sato, M. (2005). Effects of inertial and kinematic interaction on seismic behaviour of pile with embedded foundation. *Soil Dynamics and Earthquake Engineering*, 25(753-762).

Towhata, I. (2008). *Geotechnical Earthquake Engineering*. Springer, Berlin.

Wilson, D.W., Boulanger, R.W. and Kutter, B.L. (1999). Lateral Resistance of Piles in Liquefying Sand. *Geotechnical Special Publication No. 88*, pp. 165-179.

van Meurs, G., van der Zon, W., Lambert, J., van Ree, D., Whiffin, V. and Molendijk, W. (2006). The challenge to adapt soil properties. Proc. 5 ICEG: Environ. Geotechnics: Opportunities, Challenges and Responsibilities for Env. Geotechnics, 2: 1192-1199.

Valsamis A., Bouckovalas G., Chaloulos Y. (2012. "Parametric analysis of single pile response in laterally spreading ground". *Soil Dynamics and Earthquake Engineering,* Vol. 34, pp. 99-100.